Placed on: Osaka City University Repository

Journal of Geosciences, Osaka City University
Vol. 47, Art. 3, p. 21-38, March, 2004

Flash Flood Potential, Mitigation, and Floodwater Resource Management Integrating Remote Sensing and GIS Technologies in Safaga Area, Egypt

Alaa Ahmed MASOUD

Tanta University, Faculty of Science, Geology Department, Tanta 31527, Egypt
E-mail: alaamasoud@hotmail.com

Abstract

In Safaga area located on the Red Sea Coast of Egypt, catastrophic flash flooding has recently become an unfailing event resulting in great havoc and extensive loss of life and property. Yet, most of the floodwater goes waste as runoff to the Red Sea and this could meet part of the water demands for a multitude of uses in this area if efficiently utilized. The present research focuses on the integration of remote sensing and GIS techniques for flash flood potentiality, mitigation, and floodwater resource management in Safaga area. The available information included topographic, geological, LANDSAT-5 TM and JERS-1 OPS remote sensing imagery, JERS-1 Synthetic Aperture Radar (SAR), and thematic rainfall and soil data. A comprehensive hydrological database was developed including the floodplain Digital Elevation Model (DEM), geologic and structural maps, spatial hydrologic datasets, and the most specific terrain parameters that have a direct impact on the flash flood creation. Special attention was devoted to optimal selection of the input data and processing parameters to properly extract the most accurate terrain information.

Decision rules were applied to the integrated information in a GIS environment. Flood risk-prone areas were mapped, suitable sites for building dams were demarcated, and highly probable sites for recharging water were located. Structural and non-structural mitigative measures were proposed that could modify the damage susceptibility and alleviate the vulnerability of the flash flood and optimally utilize its water resource on sound scientific bases. Further, several rainfall-runoff analysis and discharge forecasting as well as flash flood inundation mapping techniques were performed to fully assess the flood potential.

Results showed good agreement with the flood hazard reports in the study area that establishes the validity of the proposed methodology for mitigating future extreme flood occurrences. This study would provide the managers and decision makers in Safaga and its neighboring areas on the Red Sea Coast of Egypt with highly accurate, up-to-date digital information and a permanent database that could provide quick and cost effective solutions for assessment and mitigation of the future flash flood events and for optimal utilization of the floodwater resources for sustainable development in these areas.

Key-words : Flash flood, Remote sensing, GIS, Safaga Area, Egypt.

1. Introduction

Egypt is one among several arid and semi-arid countries that faces the flash flood and water scarcity hazards. It is beginning to outstrip available water supply due to its increasing population, coupled with limited water resources and attendant increases in need for water. There is an urgent need to secure and utilize new supplies of water in order to sustain a minimum

resource base. Yet, catastrophic flash flooding has recently become very common in the Red Sea areas, particularly where storms hit large settlements. In these areas, flood protection cannot be provided resulting in great damage to life and property. Such floodwater can be an important renewal source of water if properly managed to meet a part of the water demand for a multitude of uses in these areas.

The development of an effective flash flood potential, mitigation, and efficient utilization of the renewable sources of floodwater in such areas become, as a consequence, more and more acute and pressing. Several efforts are needed to avert the expected crisis and a holistic perspective should be taken and integrated solutions sought for a preventive and curative plan to avoid potential conflicts that might arise because of these water-related extreme events that could help better disaster management and control. Such a perspective includes a multitude of tasks and responsibilities, such as mitigation, preparedness, and reconstruction. This can be met if new technologies, analytical tools and hydrological modeling approaches are rapidly assimilated into the understanding and management of such natural hazards.

Rapid advances in computer, remote sensing, GIS, and the spatial data management coupled with the increasing availability of digital geographic information, offer an unprecedented opportunity to harness the potential of such technology integration for computer modeling of the environment to improve our understanding and management of mountain regions (Burrough, 1986; McCullagh, 1988; Moore *et al.*, 1991). Such integration can provide the appropriate platform for hydrological modeling and integrated analysis of diverse data sets for decision making in flash flood risk assessment and water resource management and planning.

The prime objective of this work is to build a comprehensive hydrological digital database and to develop and validate methodologies allowing accurate modeling and analyzing the landscape hydrologic characteristics that could serve flash flood potential, mitigation, and optimal utilization of the floodwater in Safaga area. Several techniques are applied for the generation of the floodplain Digital Elevation Model (DEM), geologic and structural mapping, and hydrologic analysis of the derived terrain information using hydrologic database in a GIS environment.

In the next sections, the study area is introduced and the methods for the floodplain height model generation are described. The geological and structural mapping performed is presented. The hydrological modeling techniques applied are explained. Results obtained are evaluated and conclusions are drawn.

2. STUDY AREA

The study area covers about 1118 km^2 and is situated in the northern part of the Central Eastern Desert of Egypt (Fig. 1). It represents the strip of the Red Sea Coastal Plain of Egypt extending from Ras Abu Soma bay in the north to Wadi Nuqara in the south as well as the mountainous area till Nile River-Red Sea waterdivide to the west. The Red Sea Coastal Highway runs parallel to the Red Sea, while the Safaga-Qena Highway (160 Km) dissects the study area running west from Safaga City on the Red Sea Coast to Qena on the River Nile.

The study area comprises essentially of a rugged mountainous terrain comprising mainly of Precambrian basement rocks including Older Granites, metagabbro complex, metavolcanics, Dokhan Volcanics, Young Gabbros, Younger Granites, post granite dyke suites, as well as Mesozoic Cretaceous sediments and the Cenozoic Tertiary and Quaternary deposits (Egyptian Geological Survey and Mining Authority, 1987 and Masoud, 1997). These ranges are intensely dissected by numerous dry valleys (wadis) initiating from the ranges country and running eastwardly to the Red Sea. El-Barud watershed, named after Wadi El-Barud, represents the largest basin in the area. The slope is mostly steep in the upper reaches of the drainage network and tends to be gentle to the east. The highest elevations reach 1446 m (Gabal Ras Barud) and the River Nile - Red Sea waterdivide runs over the high peaks of the mountain ranges.

The area is occasionally subject to heavy rainfall during the winter season from November to January, followed by sporadic torrential floods resulting in great havoc and excessive loss of life and property in the settled urban areas and on the road network. Flash floods originating from El-Barud watershed are by far the most destructive phenomena in the study area that relies greatly on the hydrologic response and the characteristics of the watershed.

3. DATA USED

A prerequisite to successfully achieve the objective is the base data upon which most of the GIS functionalities could be built. Unfortunately, there is a lack of such data, except for topographic contour maps of scale 1:50,000 (Egyptian General Survey Authority, 1989), a

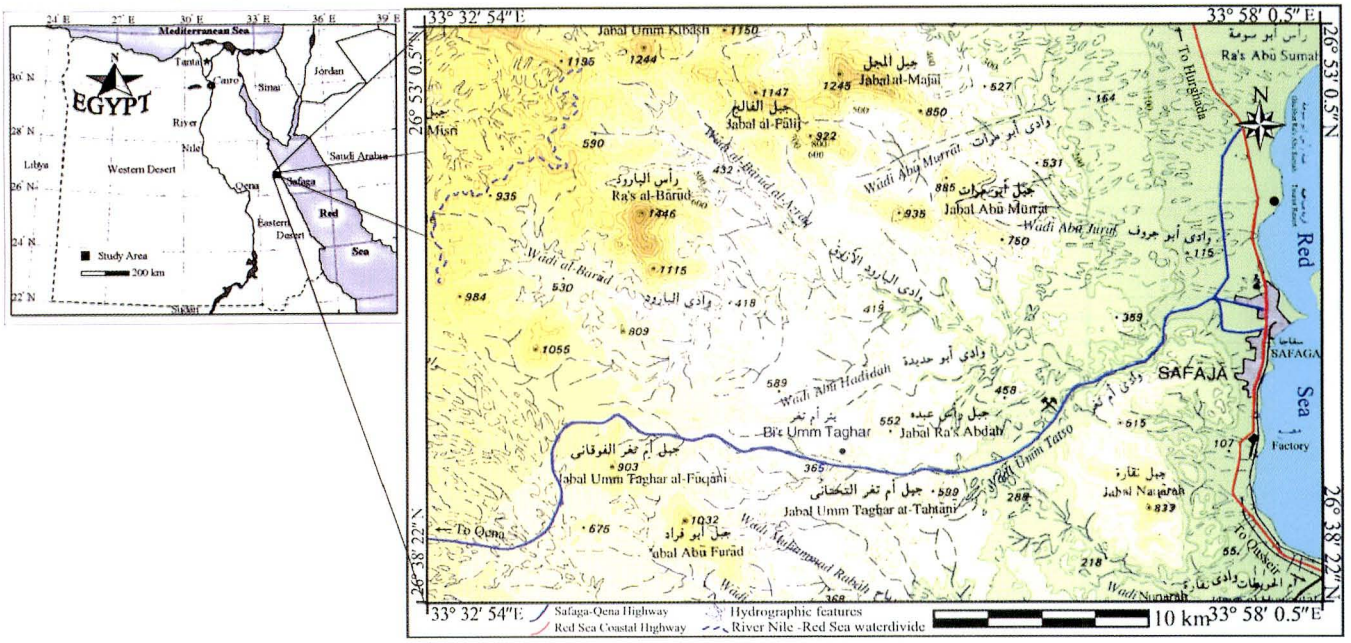

Fig. 1 Location map and topographic map of the study area (Modified after Egyptian General Survey Authority, 1996).

geological map of scale 1:100,000 (Egyptian Geological Survey and Mining Authority, 1987), and a geological map prepared by Masoud (1997). In addition to these data, a set of remote sensing imagery data as well as rainfall and soil data covering the study area have been utilized including:

1- The multispectral LANDSAT-5 *Thematic Mapper* (TM) data acquired on 14 June 2000, spatially resampled from two adjacent scenes (*Path* 174, *Row* 041-042) through cubic convolution to 28.5 m pixel size.

2- The Japanese Earth Resources Satellite-1 (JERS-1), Optical Sensor (OPS) satellite data acquired on 22 March 1996 (*Path*: 254, *Row*: 256) with a spatial resolution of 18 m pixel size and spectral range from visible green, red to near-IR, and Synthetic Aperture Radar (JERS-1 SAR) microwave data.

3- Rainfall datasets have been extracted from the Global rainfall database of 1 Degree Daily coverage (GPCP, 2003). Soil properties and its spatial distribution are extracted from the Soil Map of the World (Global Soil Data Task, 2000). The data are given in an equal-angle lat/long grid that has a spatial resolution of 1 x 1 degree lat/long.

4. METHODOLOGY

The methodology adopted in the present study is simplified and presented schematically in Fig. 2 and described in the following sections.

5. DEM GENERATION

The study area height model is generated at 28.5 m spacing integrating height information depicted on the inter-contour areas of 1:50,000 scanned topographic maps covering the study area using Horizon2000 (Shiono *et al.*, 2001) and from the InSAR processing of different L-band repeat-passes JERS-1 SAR data sets utilizing GAMMA SAR interferometry processing system (Werner *et al.*, 2000).

5.1. DEM generation from topographic maps

Terrain elevation observations are derived from four scanned topographic sheet maps of scale 1:50,000 (Egyptian General Survey Authority, 1989) covering the study area. Each scanned map is subsequently edited to retain its continuous contour lines and their inter-contour areas. Horizon2000 algorithm (Shiono *et al.*, 2001), a FORTRAN program revised from BASIC program (Shiono *et al.*, 1987), is used to build the DEM. The algorithm is based on penalized least square approximation through iteration using an exterior penalty function method (Zangwill, 1967) that works on the height information constrained in the inter-contour areas (Noumi *et al.*, 1999). Horizon algorithm has been applied to the scanned topographic maps and a 28.5 m DEM is generated. Further information on how DEM

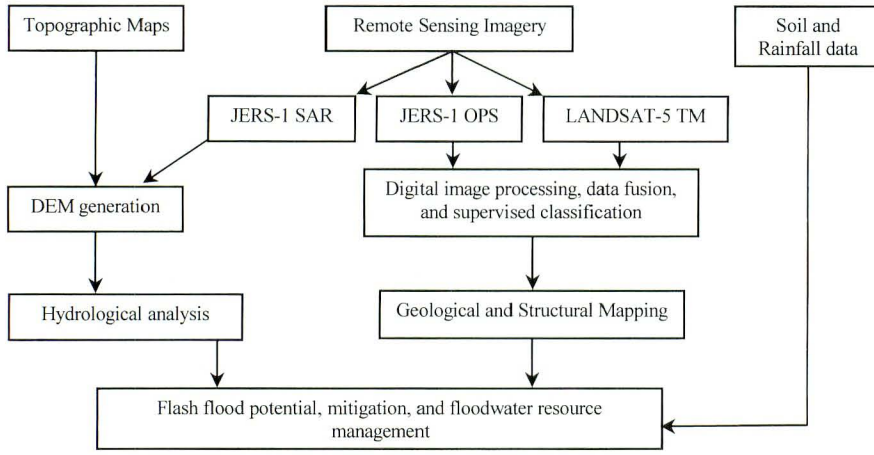

Fig. 2 Diagram showing the methodology and work-flow of the present study.

is generated for Safaga area using Horizon2000 is described in detail in Masoud *et al.*, 2002a&b. The final DEM reasonably approximated the source height data and proved efficiency to simulate the original topographic map with a root mean square Error of 2.8 m.

5.2. DEM generation from SAR Interferometry

Repeat-pass Synthetic Aperture Radar Interferometry (InSAR) is also used to generate the DEM. The whole chain of InSAR processing includes the selection of appropriate input data with minimal temporal and suitable spatial separation, single-look complex (SLC) generation, image co-registration, interferogram generation, coherence estimation, phase unwrapping, phase to height conversion, geocoding, and height model validation. Details related to the technique of InSAR processing can be found in Gens and Van Genderen (1996).

The basic requirements for InSAR are terrain of sufficient and stable backscatter, without or only with very slow changes, in the order of L-band wavelength between two passes in case of JERS-1 SAR, similar atmospheric conditions during the acquisitions, stable viewing geometry with suitable baseline, preservation of inherent phase information within the SAR processor.

Various aspects to achieve the accuracy and the quality desired for the interferometric products have been considered such as optimal data selection and processing parameters in terms of performance, accuracy and time. Constraints such as coherence, phase unwrapping, and baseline are all balanced optimally.

Based on these constraint conditions, three different datasets are selected with minimal temporal decorelation and suitable baseline lengths.

SAR processing is carried out on the three different JERS-1 raw data using the commercially available software package GAMMA SAR processing system (Werner *et al.*, 2000). Flow chart showing the GAMMA SAR processing chain for the production of an interferometric DEM is shown in Fig. 3. In the first stage of processing, each raw data scene is converted into an SLC (single-look complex image). In the second stage, these SLC's are aligned and their relative phase differences are calculated at each pixel to produce an interferogram. Three interferograms are generated coupling the three processed datasets. In the Phase Unwrapping and Height map generation stage, the relative phase differences are summed across the scene to compute overall differences. Because the satellite positions are at different angles to the surface, these phase differences will be translated into elevation differences and finally to height model.

The resulting height models are then georeferenced above the Helmert 1906 ellipsoid and Old Egyptian 1907 datum, zone 36 and have been validated using their corresponding height information of the ground control points utilized to precisely estimate their baseline as well as the reference Horizon DEM (Table 1). Results showed that the height estimation accuracy accomplished from such pairs are largely dependent on the baseline and the estimates are good enough for the first two pairs while for the third pair, although the temporal decorrelation is minimum with 44-day return period large baseline length (1050.81 m) hindered accurate height derivation for the terrain. The histogram showing the height difference of InSAR DEMs is shown on Fig. 4. Visual interpretation included comparisons of terrain profiles across the two DEMs consistent with the reference DEM. The profiles showed quite good correspondence particularly where the rate of change in local relief is relatively low; with large height estimates deviations are confined to the steep slope areas away

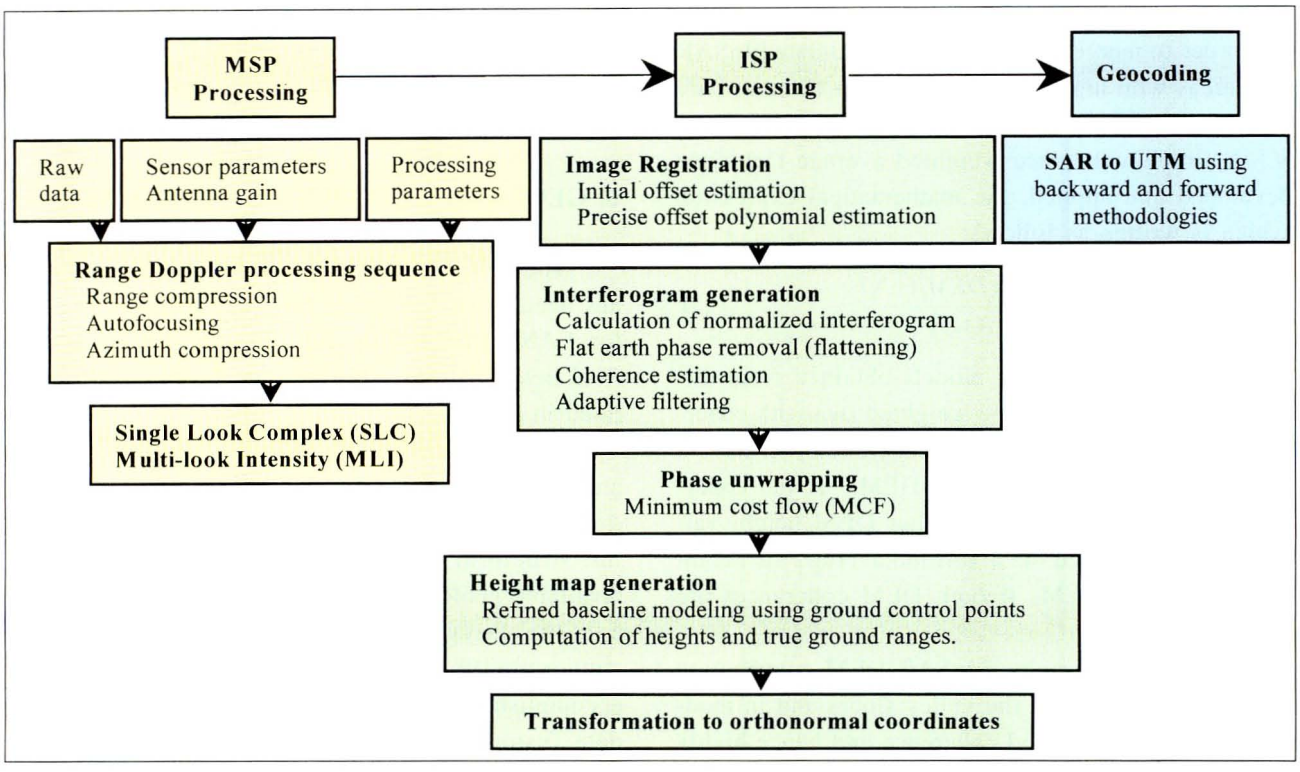

Fig. 3 GAMMA SAR processing chain for interferometric DEM generation.

Table 1 Baseline characteristics of the three processed interferomtric pairs and their DEM evaluation.

Interferogram Pair	94-01/96-04	94-01/96-06	96-04/96-06
Orbital baseline length (m)	495.50	757.63	1134.21
GCP-based baseline length (m)	334.18	728.98	1050.81
GCPs	32	35	73
GCP-based RMSE (m)	9.060	9.40	26.19
Horizon DEM-based RMSE (m)	11.96	12.20	34.6

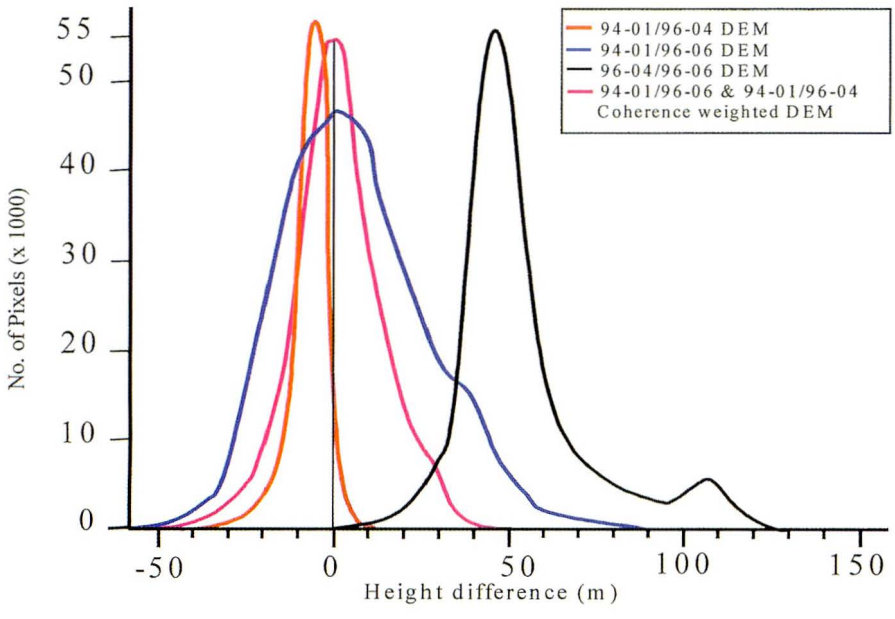

Fig. 4 Histogram of the height differences.

from SAR where coherence is evidently low.

In order to merge the merits of the validated InSAR DEMs, areas with highest accuracy height estimates are preserved and used to build a DEM with enhanced accuracy. A simple coherence weighted average technique is developed and applied, the mathematical expression of which is written as follows:

$$DEM_f(x, y) = \frac{\sum_i w_i(x, y)\, DEM_i(x, y)}{\sum_i w_i(x, y)} \quad (1)$$

DEM_i stands for height models obtained from different image pairs. DEMs are weighted (w_i) with coherence, *i.e.* the model with higher coherence will have a stronger contribution to the final DEM. If the coherence of one model is zero, the other DEM height values will be selected and the algorithm average the height values of the two DEMs if both DEM coherences are zero.

The coherence weighted InSAR DEM contribution was especially evident in the valley floors and in moderate relief areas with good coherence and hence highly accurate height estimates with RMSE of 8.64 m is achieved. The merits of both the reference horizon DEM and the final InSAR DEM are then combined to produce a final DEM (Fig. 5). The horizon DEM is used to verify the InSAR final DEM in areas of larger height errors and is expected to increase the vertical accuracy of the final DEM.

6. GEOLOGICAL AND STRUCTURAL MAPPING

The geological and structural map of the study area has been produced integrating digital image processing for LANDSAT-5 TM and JERS-1 imagery data and field investigations. The proposed methodology is outlined in Fig. 6.

Field work has been carried out in December 2001 and January 2002 to investigate the distribution of the different lithologic units, their interrelationships, and the structural patterns dominant in the study area. Available geological maps produced by Masoud (1997) and the Egyptian Geological Survey and Mining Authority (1987) have been used as source base data for accomplishing this task. Further, several enhancement, data fusion, and classification techniques on LANDSAT-5 TM and JERS-1 optical sensor imagery have been applied to infer the geological and structural attributes of the area under consideration. Data processing,

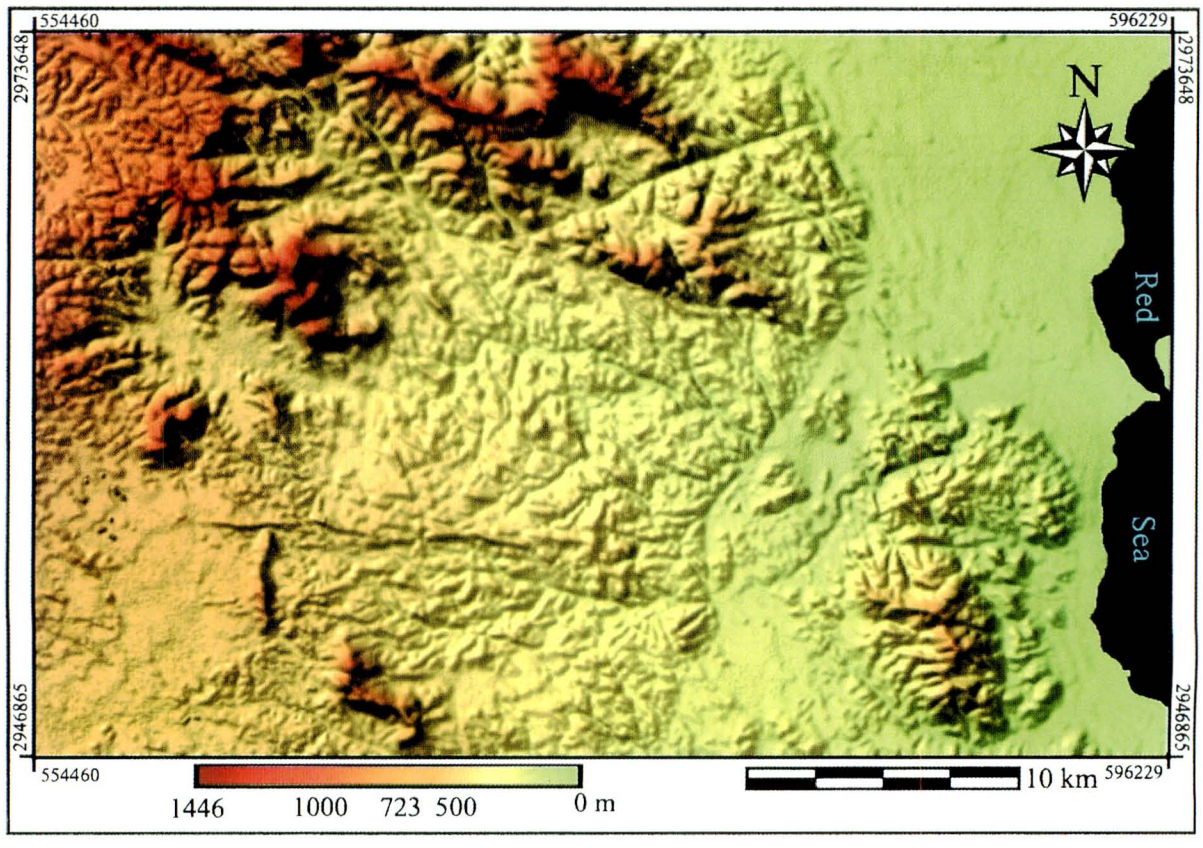

Fig. 5 Shaded relief map of the final DEM integrated from Horizon and InSAR DEMs.

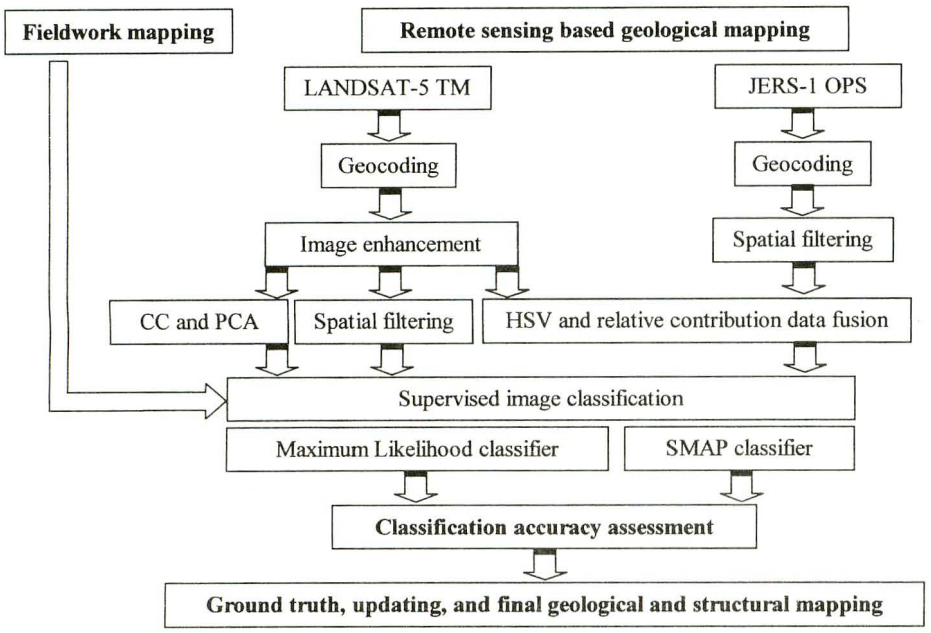

Fig. 6 Methodology and data processing.

classification algorithms, and evaluation techniques have been performed within GRASS GIS (GRASS Development Team, 2003).

The acquired LANDSAT-5 TM and JERS-1 OPS data are georeferenced to UTM map coordinates, zone 36, Helmert 1906 ellipsoid and the Old Egyptian 1907 datum based ground control points (GCP) extracted from radar intensity images generated utilizing SAR interferometry techniques. A sub-scene covering the area of interest has been selected for further processing and classification of the geologic and structural-related features.

Several image processing techniques have been applied for the TM and JERS-1 bands of the sub-scene including statistical analysis, spectral enhancement (color composites, principal component analysis, and spatial filtering), data fusion, and image classification.

Two supervised classification techniques, maximum likelihood classifier and a *sequential maximum a posteriori* (SMAP) implemented in GRASS GIS, are applied to extrapolate the detected spectral features into a geological map. Training classes derived from the available geological maps, field investigations, and from the processed data are used to train the classification program to recognize spectrally similar areas for each class.

The two classification procedures are applied for the color composites and the PCA generated from the original TM data, the filtered data, and the fusion-estimated data. Applying these techniques, 12 rock varieties have been identified and classified. The accuracy of the classification has been evaluated using the Kappa Coefficient technique (Congalton, 1991) and shown on Table 2. The geologic map produced from SMAP technique has proved promising and has been rechecked through ground truthing and the contacts of the geologic units are verified. In addition to the classified lithologic maps, the structural patterns are easily derived from such enhanced and fused products. A final geological map with the detected structural attributes and the tectonic implications of different rock units is shown on Fig. 7.

7. FLASH FLOOD POTENTIAL, MITIGATION, AND FLOODWATER RESOURCE MANAGEMENT

DEM has been analyzed to delineate the watershed boundary and its stream networks as well as the most important hydrologic parameters that have a direct impact on the flash flood creation. These data as well as the geological and structural map have been integrated with the soil data and the rainfall records to evaluate the flood potentiality allowing mitigation measures to be proposed and for investigating the suitability for efficient utilization of the floodwater. Further, rainfall-runoff analysis and physically based distributed hydrological modeling approaches have been applied that could be used as predictive tools for flash flood occurrences.

7.1. Watershed and stream modeling

A watershed basin analysis algorithm, *r. watershed*,

Table 2 Classification accuracy of the detected classes from the original, filtered and the fused CC and PCA data.

% Coverage and Classifier used	Coverage %	Maximum Likelihood classifier			SMAP Classifier		
Data / Classes		CC and PCA	Filtered CC and PCA	Filtered TM and JERS_1 fused	CC and PCA	Filtered CC and PCA	Filtered TM and JERS_1 fused
Red Sea	4.76	0.980	0.980	0.987	0.982	0.982	0.988
Quaternary deposits	30.62	0.665	0.681	0.699	0.704	0.701	0.718
Tertiary deposits	0.94	0.596	0.594	0.692	0.748	0.752	0.789
Cretaceous deposits	0.25	0.465	0.420	0.571	0.563	0.511	0.672
Younger Granite G2.2	2.10	0.551	0.632	0.707	0.719	0.726	0.779
Younger Granite G2.1	3.43	0.509	0.548	0.706	0.718	0.677	0.823
Younger Granite G1.2	14.45	0.312	0.331	0.482	0.548	0.497	0.615
Younger Granite G1.1	4.69	0.700	0.803	0.826	0.860	0.889	0.898
Young Gabbros	0.39	0.551	0.570	0.659	0.766	0.698	0.771
Acidic Dokhan Volcanics	3.63	0.692	0.690	0.727	0.757	0.717	0.764
Intermediate Dokhan Volcanics	2.26	0.477	0.555	0.585	0.556	0.637	0.660
Older Granites	33.89	0.254	0.337	0.421	0.456	0.485	0.552
Metagabbro	2.78	0.663	0.705	0.754	0.765	0.759	0.808
Total Kappa		0.488	0.536	0.606	0.633	0.632	0.690
% Correct		56.27	60.78	67.04	69.38	69.44	74.42

implemented in GRASS GIS (GRASS Development Team, 2003) and Strahler stream ordering algorithm (Strahler, 1952) implemented in TauDEM (Tarboton, 2002) have been appraised to delineate the watershed boundary and its stream channel networks processing the integrated DEM. Applying this program to the DEM, watershed and its topographic hydrologic properties were delineated and many key products such as flow accumulation, flow direction, slope length, and slope steepness maps were generated. The extracted streams of different orders in El-Barud watershed and its delineated boundary are shown overlaying the LANDSAT-5 TM enhanced data that provided a good matching and corresponding to the boundary and the stream networks locations (Fig. 8).

7.2. El-Barud geomorphologic and morphometric characteristics

It is generally accepted that runoff resulting from rainfall is dictated by compositional characteristics of the drainage basin that can be described by empirical laws of geomorphology (Horton, 1945; Strahler, 1957; Smart, 1972), at least in the shape of the hydrologic response. Geomorphologic and morphometric characteristics (such as total drainage segment number, total network length, network frequency, and density, etc.) and drainage basin characteristics (basin area, slope, perimeter, roughness, elongation, relief ratio, ruggedness number, shape index aspect, circularity, etc.) are estimated from the DEM in GRASS GIS for El-Barud watershed and shown on Table 3. All basin characteristics except for basin relief ratio were calculated as reported in Harvey and Eash (1996), using GRASS GIS. Basin relief ratio was calculated using methods outlined in Fitzpatrick *et al.* (1998) and Schumm (1956).

El-Barud watershed showed a high drainage density with high bifurcation ratio and frequency indicating the potential of the basin for runoff and high flash floods response. The dendritic (tree-like) stream pattern facilitates more rapid concentration of runoff at or near the watershed's outlet; this increases the likelihood of downstream flooding.

All of the physiographic characteristics of the basin support the potentiality of the basin for flash floods and the floodwater discharge. Large watershed coverage, relief, and the shape attributes indicate low infiltration rate, large runoff volumes, short overland flow, and high risk of flash flood.

7.3. Wetness Index and artificial well recharging

Wetness index (WI) has proved to be very useful in calculating runoff hydrographs for upland catchments (Beven and Kirkby, 1979; O'Loughlin, 1981; Moore *et al.*, 1991; Wolock, 1993). Wetness Index sets catch-

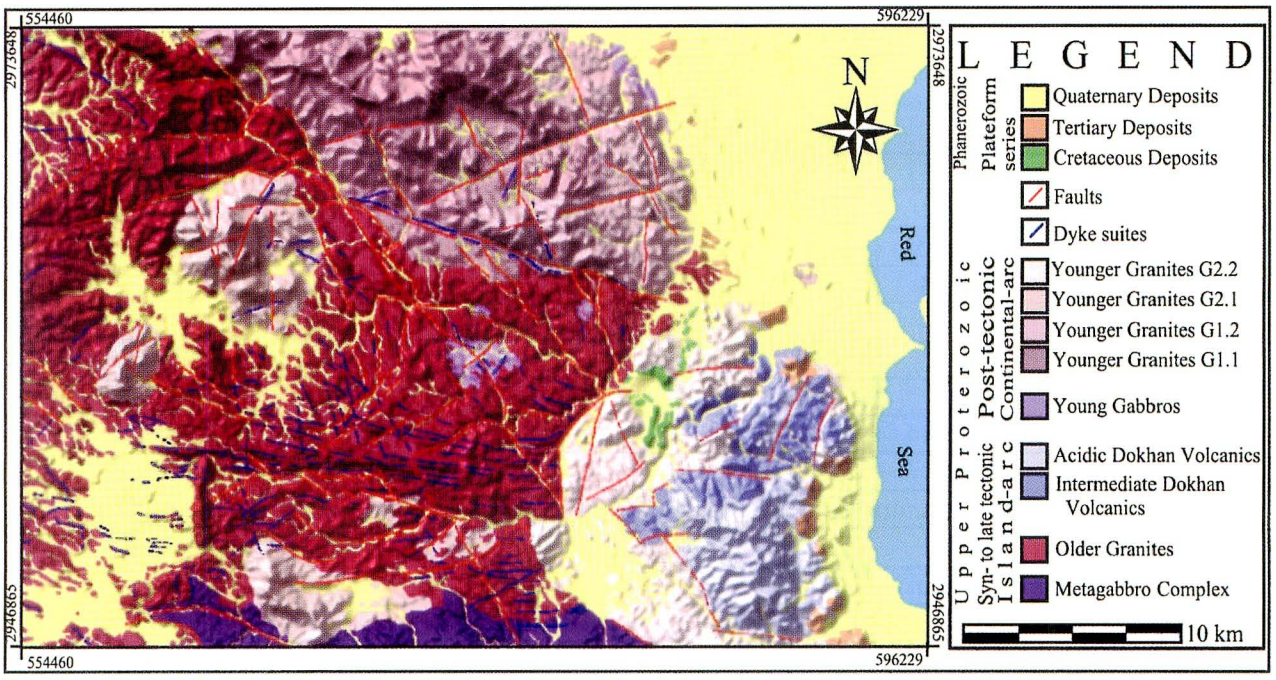

Fig. 7 Geological map draped over DEM showing distribution of the different lithotypes and detected structural features and their tectonic implications.

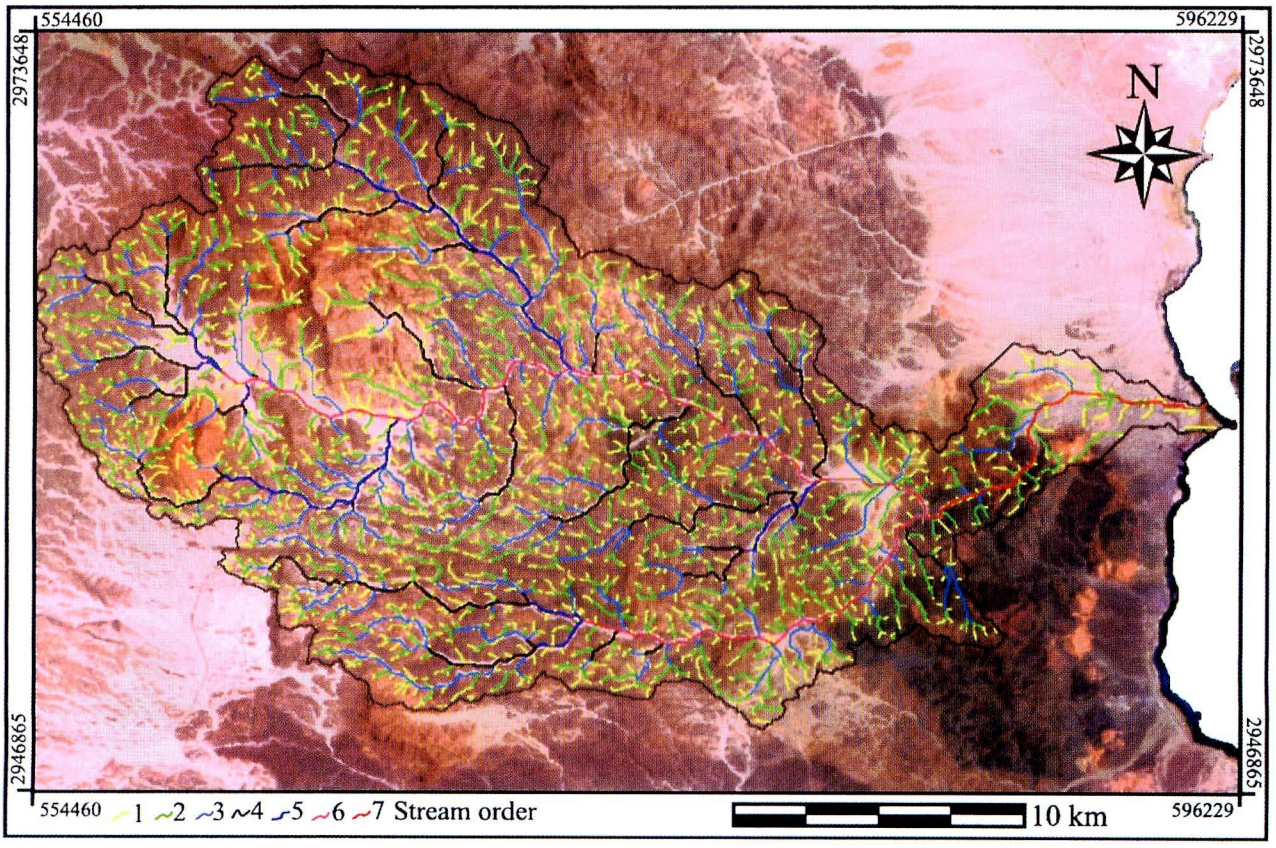

Fig. 8 El-Barud watershed and its stream network overlaying the remotely sensed enhanced data covering the study area.

Table 3 Morphometric and geomorphologic characteristics of El-Barud watershed and its stream network.

	Stream Order	No. of Streams	Length of streams (km)	Area Cov. km^2	Drainage density (km/km^2)	Stream frequency ($1/km^2$)	Horton's ratios R_B	R_L	R_A
Morphometric parameters	1	1631	666.85	15.73	1.35	3.32	2.63	1.72	1.72
	2	619	386.06	9.11	0.78	1.26	3.99	1.54	1.53
	3	155	250.89	5.92	0.51	0.31	5.53	2.21	2.21
	4	28	113.31	2.67	0.23	0.057	3.5	3.25	3.26
	5	8	34.68	0.81	0.07	0.016	4	0.7	0.7
	6	2	48.85	1.15	0.09	0.004	2	3.42	3.47
	7	1	14.06	0.33	0.02	0.002			
	Total	2444	1514.73	35.75	3.08	4.97	3.6	2.14	2.14

	Watershed Parameter	Value	Watershed Parameter	Value
Geomorphologic parameters	Area (km^2)	491.74	Main channel slope (°)	12
	Perimeter (km)	185.76	Shape factor	1.89
	Watershed length (km)	40.28	Form factor	0.168
	Watershed width (km)	21.25	Circularity ratio	0.18
	Watershed relief (m)	1440	Elongation ratio	0.62
	Watershed relief ratio	0.035	Compactness coefficient	2.36
	Main channel length (km)	54.966	Ruggedness number	4.43
	Watershed slope (m/m)	0.0166		

ment area in relation to the slope gradient. This is basically expressed as:

$$WI = \ln\left(\frac{A_s}{\tan(\theta)}\right) \quad (2)$$

Where A_s is the area drained per unit contour or the specific area, and $\tan(\theta)$ is the slope. Regions of the landscape that drain large upstream areas or that are very flat give rise to high values of the index; thus areas with the highest values are most likely to become saturated during a rain event and thus are most likely to be areas that contribute surface runoff to the stream. The watershed wetness index is calculated for the watershed using *r. topidx* module in GRASS GIS. During field investigations conducted in November 1994 and December 2000 and January 2001, three productive wells were recorded and are in use by local Bedouin tribes for watering camels, goats and for human use. The well sites are analyzed with the wetness index map generated from DEM and it was concluded that these sites have a *WI* of 18. Based on this, all sites greater than this reference value are identified and located. Ninety-nine sites have been extracted and integrated with the basin geology and the structural attributes within GIS environment to demarcate sites with high probability for recharging wells. Sites that are located within the alluvial and wadi deposits and 300 m near to dyke structures are proposed to have high potentiality for the subsurface storage of the floodwater. Fifty-four sites met these conditions and reclassified according to their *WI* from 1 to 10 ranks. Fig. 9 shows the demarcated sites and their corresponding probability for recharging well. Such a technique can help in exploitation of floodwater for recharging near-surface aquifers in arid terrains and other neighboring areas in the Red Sea hydrographic basin that can in turn make resources available as sustainable water management at the watershed level.

7.4. Flash flood potential and mitigation

A landuse map with the residential areas and roads located within the area under investigations is digitized in a raster format from the remotely-sensed enhanced data. Road network is classified into three categories, Safaga-Qena highway, Red Sea Coastal highway, and the city infrastructure roads. The analysis of such landuse maps with the derived hydrological products as well as field investigations in the flood plain under concern, showed that about 7 km^2 residential areas located at the watershed outlet are prone to flash flood risks (Fig. 10). Numerous physical injuries are possible, and public infrastructure and private property may be dam-

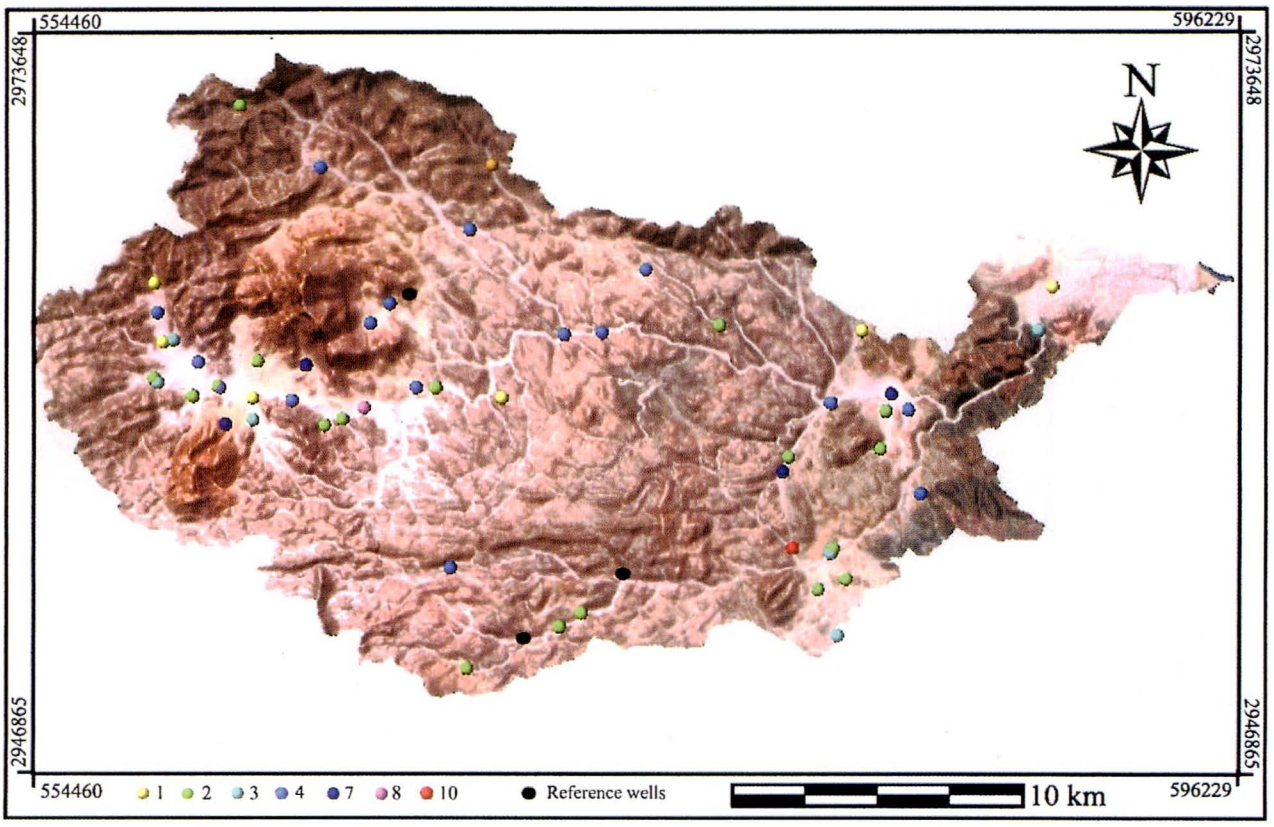

Fig. 9 Demarcated well sites suitable for recharging water with their probability index within El-Barud watershed.

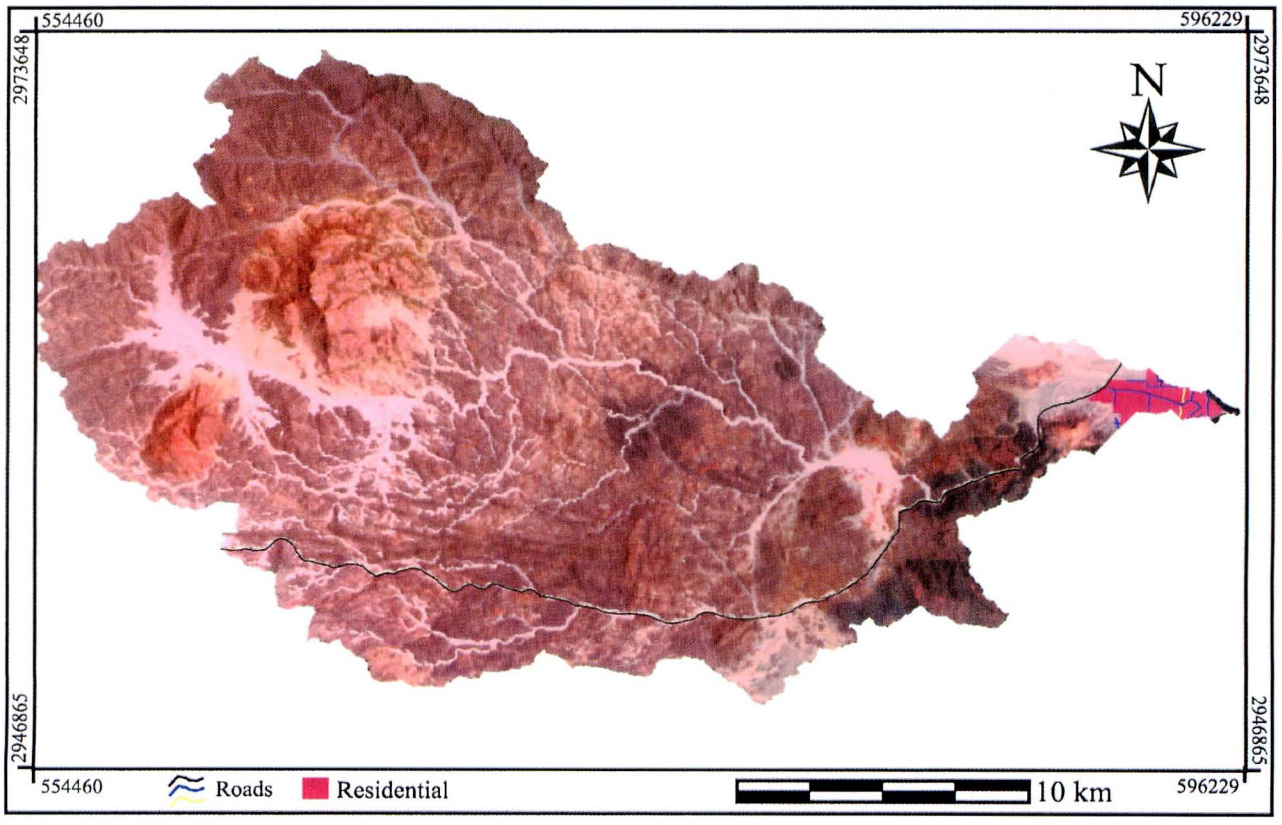

Fig. 10 Flash flood risk-prone landuse units of El-Barud watershed.

aged with inundation. In addition, 47.3 km of the road network including 38 km (Qena-Safaga highway), 8.3 km (city roads), and 1 km of the Red Sea Coastal highway are located within the watershed and are vulnerable to flash flood risks that may be washed-out in floods.

Further field investigations indicated that expanding urbanization at the watershed outlet is among the major contributing factors to the flood vulnerability. This is because impervious surfaces such as roofs and roadways compact the soil and reduces infiltration rates. Also, the ground floors at the outlet are gently sloped, poorly drained, not elevated more than about 1 meter above ground level, and the buildings are not properly anchored to their foundation that can be washed-out and swept away during flooding. Furthermore, major disruptions of the road network are activated by the absence of suitable bridges and culverts where the main streams meet these roads. The properties therefore provide little attenuation of the rainfall amount or little retardation of the travel of the flood volume toward the low-lying areas.

To assess flash flood risk at roadway crossings in the study area, an approach has been adopted, that is based on the flow accumulation at the stream-roadway crossings since the intersections represent risks at routes of evacuation and support development design and emergency response decision-making. Flash flood potential on the road networks are assessed using the flow accumulation map previously generated from hydrological analysis of the DEM. The road sites that receive higher water accumulation will have a higher probability for washing out through the flood. The flow accumulation values along the roads are classified from 1 to 10 probability ranks, with the highest risk zones designated as 10. Based on this scale, two hazardous zones are classified, namely, slightly hazardous zones and highly hazardous zones. Fig. 11 shows the flood hazard probability spatial distribution for the road network and their hazardous zones. The resulting model showed that the highly vulnerable at-risk sites along the roads with a probability of 10 are those located at Km 10 from Safaga city and those at the mouth of the main wadi within the city. This was reported in Raafat Masak (1991) who stated that flash floods have swept away blocks from the Safaga-Qena highway at Km 10 from Safaga City and which interrupted the traffic along the road to Qena. Also, the highly hazardous zones identified are comparable with the results reported in Ashmawy (1994). These results establish the validity

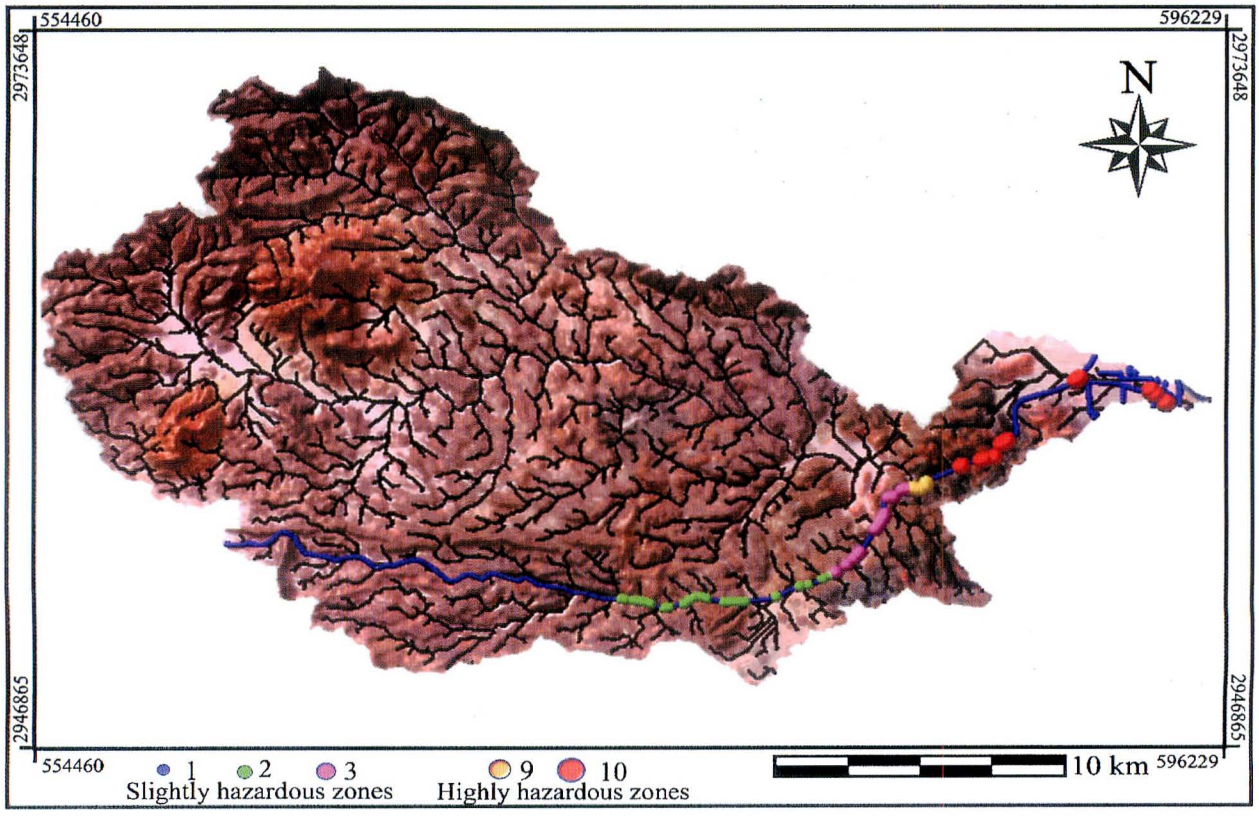

Fig. 11 Road network flash flood vulnerability index map.

of the flow accumulation information for zoning the hazardous road sectors within the floodplain.

Based on the findings revealed from flash flood risk zone maps, preventive structural and non-structural measures should be considered to help modify susceptibility to flood damage or the impact of flooding. Structural measures include constructing dams and reservoirs, ditches, and culverts and non-structural measures involve zoning, *i.e.* regulation for flood hazard areas development leaving floodplains with low-value infrastructure. Constructing dams and reservoirs where the excess water can be stored allows a regulated temporal distribution of stream flow and helps alleviate the flood problem by flattening flood peaks.

Site suitability for building dams on the main wadis and the active tributaries are investigated through demarcating locations where stream channels meet the roads that have a high runoff and are proposed to have a high priority for building dams. Further, sites just behind the proposed artificial wells located within the alluvial deposits with a width of about 35 m are selected as sites for dam building. Such decision rules may serve the double goal of reducing the flash flood risks as well as storing and regulating water for domestic uses. Fig. 12 shows the proposed dam sites in El-Barud Basin.

Structural measures for alleviating the flood risks along the road sectors could include constructing artificial channels (ditches), in particular, at narrow steep slope sites, building diversion canals at the areas of crossing of main courses with road network, as well as large enough culverts near the mouths of the main wadis at the coastal plain.

Non structural measures related to planning and hazard mitigation include zoning flood prone areas as at-risk zones, prohibiting new settlements, and developing appropriate standards for acquiring or elevating structures in the most flood prone areas. Further, implementing a variety of flood control policies to all new construction to prevent flotation, collapse, or lateral movement of the structure during flooding. Furthermore, developing a screening process for hazards prior to development in floodplains, and implementing and encouraging "best management practices" related to flash flood management to lessen its problems.

7.5. Rainfall-runoff analysis

Major factors that affect the runoff volume and associated peak discharge are the rainfall duration and intensity, soil types in the watershed, and the time of concentration (Haan *et al.*, 1982; Chow *et al.*, 1988).

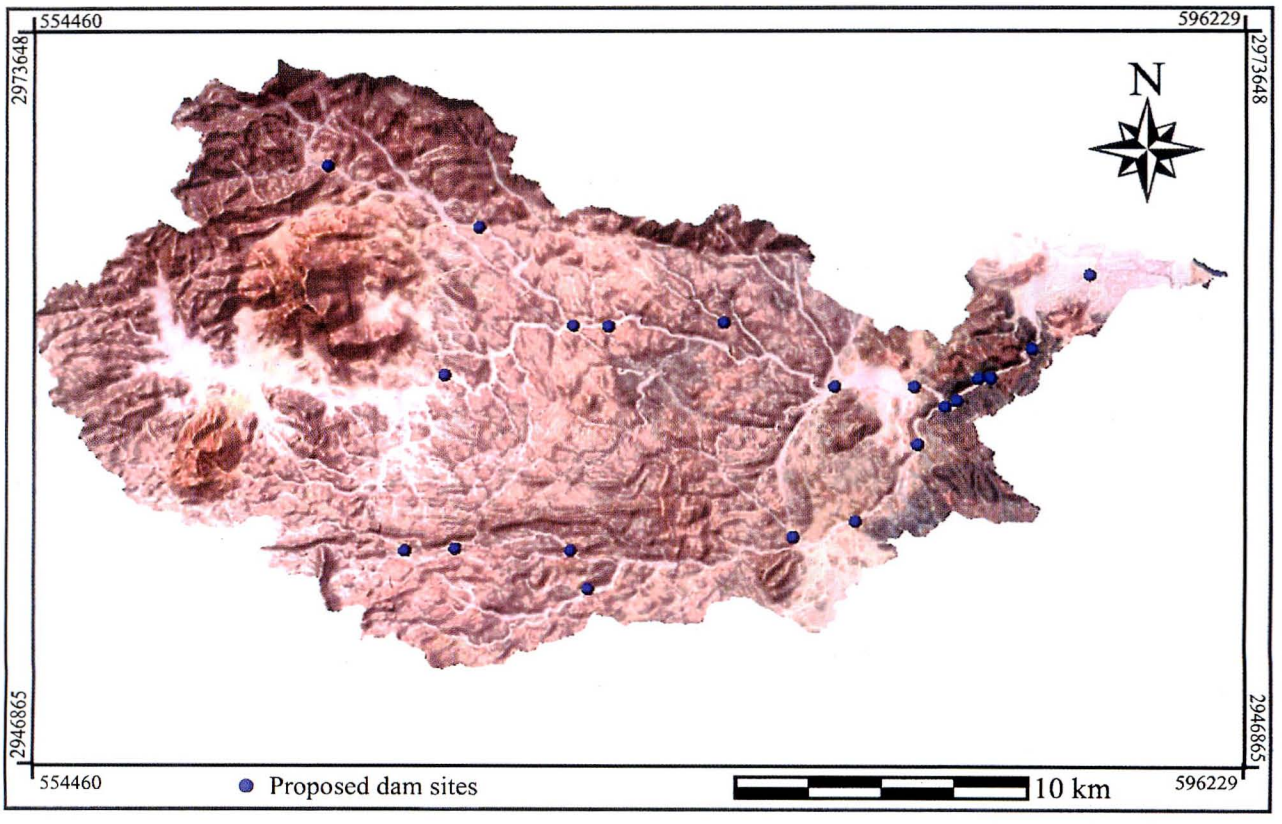

Fig. 12 Proposed dam sites in El-Barud watershed.

Several techniques have been available for the estimation of runoff volume and peak discharge ranging from simplified procedures for homogenous areas, to complicated algorithms that can handle more complex situations. The simple synthetic unit hydrograph methods utilizing the Snyder's (Snyder, 1938) and the SCS triangular unit hydrograph method (U.S. Soil Conservation Service (SCS), 1972) as well as the SCS curve number technique (USDA-SCS, 1985) have been appraised and adopted to calculate runoff characteristics at the El-Barud watershed outlet increasing the cost of the flash flood vulnerability. Such a technique represents a substantial first step and framework from which to build an effective flash flood prediction tool.

The rainfall-runoff characteristics for El-Barud watershed applying these techniques are shown on Table 4. Peak discharges from the applied techniques are in harmony giving an average of 46 m^3/s and 20 hour for time to peak. This is a substantial rate of runoff that could be an important renewal source of water for a several domestic uses. It would also be sufficient for an effective in-time warning and evacuation system to be set up in the Safaga area. El-Barud Unit hydrographs applying Snyder's and the SCS triangular techniques are shown in Fig. 13. With these unit hydrographs, there is a possibility to examine the basin response to various storm events. Once actual field data is collected for storm events, calibration of this model can take place. Subsequently, a representative model of the watershed can be built. From that point, further analysis of the watershed can proceed with better predictive capabilities.

7.7. Flash flood inundation modeling

In order to simulate the flood event and to map the areas that were inundated during flash flooding on Safaga city, an integrated physically-based hydrologic model consisting of various hydrological components and governing equations for flow propagation (Dutta *et al.*, 2000a & b) have been adopted and applied in the study area using rainfall records for the period 5 - 28 October 1997. This period is selected based on a report published by Shohami (1997). This modeling technique has been applied to many river basins in Japan and proved efficient in basin scale flood simulation. Field investigations and interviews with the Safagan people proved that the water level reached about 4 m in some parts of the city.

The model hydrological components are a) interception and evaporation, temporal rainfall data and spatial landcover distribution, b) river flow, temporal upstream and down stream boundary conditions with water level and discharge information, and spatial river network, channel cross-section, and roughness factors, c) overland flow that requires DEM and the surface roughness coefficient, and d) unsaturated subsurface zone, spatial soil types and hydrologic properties with the initial soil moisture parameters.

Comprehensive digital datasets have been prepared including spatial, temporal and other parameter data. The spatial data included DEM, soil distribution and its hydraulic characteristics, landuse map, river network and flow accumulation map. Soil properties and its spatial distribution are extracted from the Soil Map of the World (Global Soil Data Task, 2000). Landuse data, in particular, the residential area are extracted from the enhanced remotely sensed fused LANDSAT-5 TM with JERS-1 OPS data. Stream channel networks and flow accumulation maps are derived from the hydrological analysis of DEM. Rainfall datasets have been extracted from the Global rainfall database of 1 Degree Daily coverage (GPCP, 2003). River width is measured applying a formula of the downstream hydraulic relationships developed by Leopold and Maddock (1993). The channel distribution and their numbers are shown in Fig. 14.

Applying the model to the data, the whole area inundated by the flash flood water is about 3.903 km^2 from which the residential areas cover 3.2877 km^2. Fig. 14 shows the flood-inundated residential areas with water level contoured at 0.5 m interval over the enhanced remotely sensed image as well as the stream channels and its codes used in the model. Table 5 shows the flash flood inundated residential areas and their corresponding water level.

Table 4 El-Barud watershed rainfall-runoff characteristics.

Parameter	Time to Peak (hr)	Peak Discharge, Q_p (m^3/s.cm)
Snyder's UH	22.82	50.28
SCS UH	22.82	43.08
SCS *CN*	17.80	44.70
Average	20.31	46.02

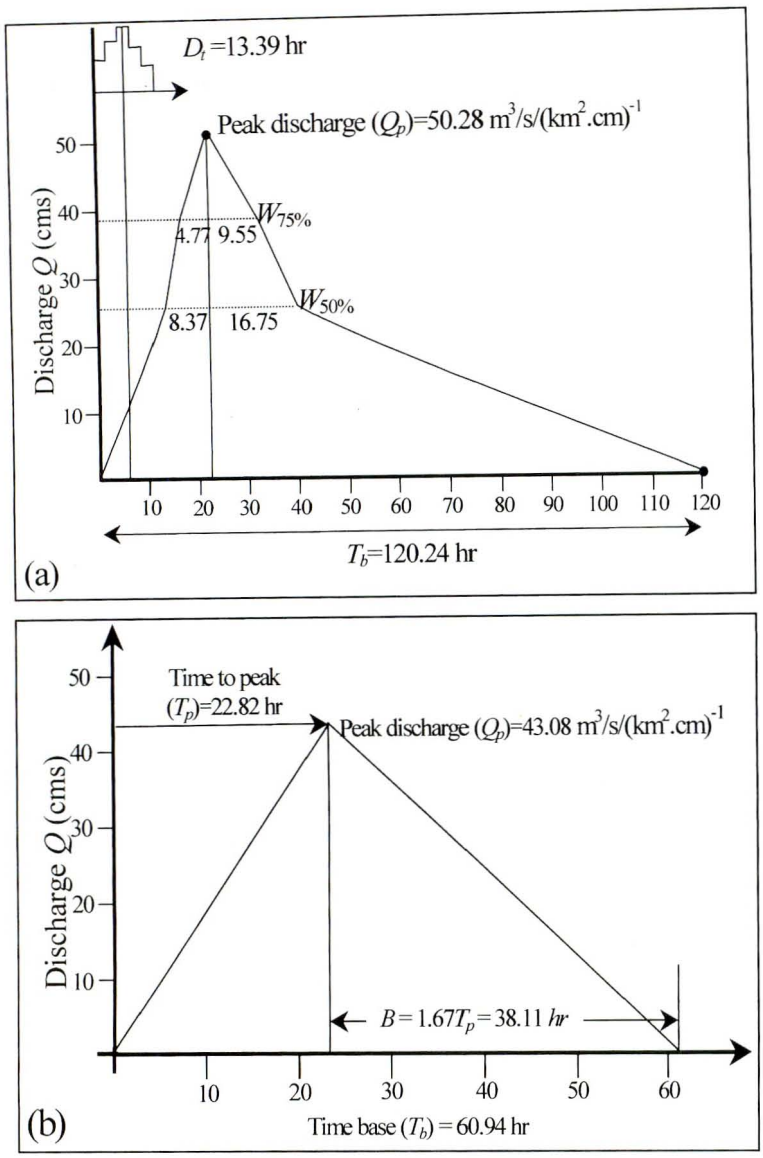

Fig. 13 The Snyder's (a) and the SCS (b) unit hydrographs developed for El-Barud watershed.

8. CONCLUSIONS

The research as discussed in this paper, is a strategy of methods for evaluating arid-land flash flood potential, mitigation, and floodwater resource management as well as a rainfall-runoff simulation model that is efficient for arid land storm runoff management. Integration of remote sensing and GIS provided the appropriate platform for hydrological modeling and analysis of diverse data sets for potent decision-making. The results of this work could provide the Safaga area's water resource managers and decision makers with highly accurate, up-to-date digital information and a spatial database. This database is easy to reproduce in various scales, easy to store, retrieve, and update in a GIS system environment and thereby eliminating the need to recreate it for future sustainable development in the area. It can be used for future projects speedily and cost-effectively and which will provide solutions for assessment and mitigations of the extreme water-related events. Also, the measures proposed could help modify susceptibility to flood damage and utilize the floodwater based on sound recent scientific bases. According to the information we have, this is the first comprehensive study that has been done in Safaga and neighboring areas. It is extremely important to apply these advanced water-related risk techniques in this harsh, fragile and arid region to evaluate water-related extreme events.

The obtained results from the proposed strategy of methods are encouraging and provide good reference for future research. More experiments and tests might be done to achieve fully operational outcomes. Therefore,

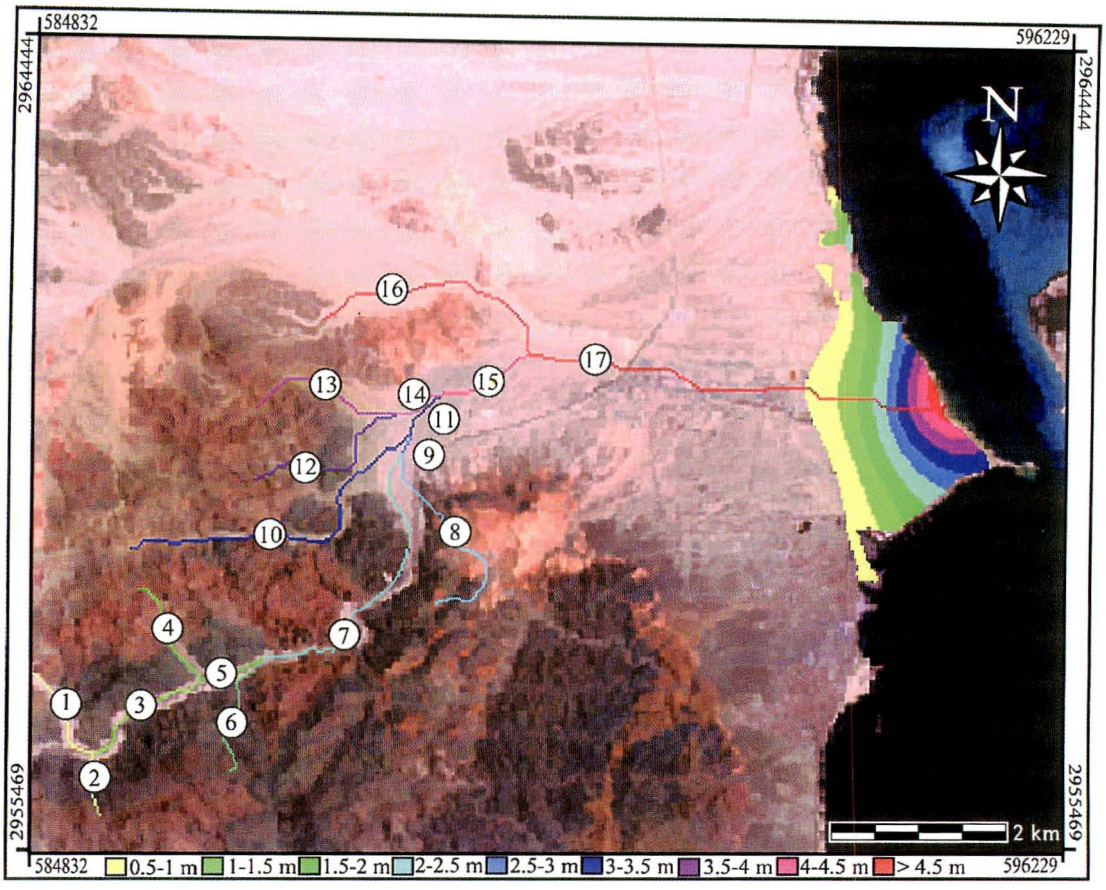

Fig. 14 The inundated residential areas with 0.5 water level interval.

Table 5 Flash flood inundated residential areas and their corresponding water level.

Water level (m)	Inundated areas (km^2)
0.5-1	0.842
1-1.5	0.609
1.5-2	0.507
2-2.5	0.378
2.5-3	0.298
3-3.5	0.282
3.5-4	0.196
4-4.5	0.130
4.5-5	0.041
Total	3.283

for future projects in this area, it might be prudent to investigate other techniques and datasets with higher resolution for DEM generation and geological mapping. With additional research, it is envisaged to incorporate temporal inputs into the models with output being given in a spatial temporal manner, and which would be more efficient and useful. R & D on this aspect in Egypt would lead to promising results already addressed and shown in this work.

REFERENCES

Ashmawy, M. H. (1994) Assessment of flash flood potential of the Red Sea drainage basins along the Qena-Safaga highway, Eastern Desert, Egypt. *ITC Journal*, **2**, pp. 119-128.

Beven, K. F. and Kirkby, M. J. (1979) A physically based, variable contributing area model of basin hydrology. *Hydrological Science Bulletin*, **24**(1), pp. 43-69.

Burrough, P. A. (1986) Principles of Geographical Information Systems for Land Resources Assessment, *Monographs on Soil and Resources Survey*, Oxford University Press, New York, 194p.

Chow, V. T., Maidment, D. R., and Mays, L. W. (1988) *Applied Hydrology*. McGraw-Hill, New York, 572 p.

Congalton, R. (1991) A Review of Assessing the Accuracy of Classifications of Remotely Sensed Data. *Remote Sensing of Environment*, **37**, pp. 35-46.

Dutta, D., Herath, S., and Musiake, K. (2000a) Flood

Inundation Simulation in a River Basin Using a Physically Based Distributed Hydrologic Model. *Journal of Hydrological Processes*, John & Sons, **14**(3), pp. 497-520.

Dutta, D., Herath, S., and Musiake, K. (2000b) Physically Based Surface-River Flow Coupled Model for Flood Inundation Simulation in a River Basin. *Proceedings of the International Summer Symposium, Japan Society of Civil Engineers*, pp. 189-192.

Egyptian General Survey Authority (1996) Topographic sheet of Al-Qusayr, scale 1:250,000.

Egyptian General Survey Authority (1989) Topographic sheets of Safaga, Ras Abu Suma, Gabal Umm Inab and Gabal Wairah, scale 1:50,000.

Egyptian Geological Survey and Mining Authority, (1987) Basement Rocks of Safajah Quadrangle, Egypt, Scale 1:100,000.

Egyptian Meteorological Authority (1994) Monthly weather reports of 1994, (Unpubl.).

Fitzpatrick, F. A., Waite, I. R., D'Arconte P. J., Meador, M. R., Maupin, M. A., and Gurtz, M. E. (1998) Revised methods for characterizing stream habitat in the National Water-Quality Assessment Program: U.S. Geological Survey Water-Resources Investigations Report 93-4052, 67p.

Gens, R. and Genderen, J. L. V. (1996) Review Article: SAR interferometry - issues, techniques, and applications, *International Journal of Remote Sensing*, **17**(10), pp. 1803-1835.

Global Soil Data Task. (2000) Global Soil Data Products CD-ROM (IGBP-DIS). International Geosphere-Biosphere Programme, Data and Information System, Potsdam, Germany. Available from Oak Ridge National Laboratory Distributed Active Archive Center, Oak Ridge, Tennessee, U.S.A. [http://www. daac. ornl. gov].

GPCP (2003) Global Precipitation Climatology Project http://precip. gsfc. nasa. gov/gpcp_v2_comb. html.

GRASS Development Team (2003) http://www3. baylor. edu/grass/ and http://wgrass. media. osaka-cu. ac. jp/grassh/index.html.

Haan, C. T., Johnson, H. P., and Brakensiek, D. L. (1982) Hydrologic Modeling of Small Watersheds. American Society of Agricultural Engineers, **5**, St. Joseph, Michigan.

Harvey, C. A. and Eash, D. A. (1996) Description, instructions, and verification for Basinsoft, a computer program to quantify drainage-basin characteristics: U.S. Geological Survey Water-Resources Investigations Report 95-4287, 28p.

Horton, R. E. (1945) Erosional development of streams and their drainage basins; hydrophysical approach to quantitative morphology. *Geological Society of America Bulletin*, **56**, pp. 275-370.

Leopold, L. B. and Maddock, T. (1993) The Hydraulic Geometry of Stream Channels and Some Physiographic Implications. U.S. Geological Survey Professional Paper, **252**, 57p.

Masoud, A. (1997) Geology and Tectonic Evolution of the Area Around Gabal Abu Furad, Northern Eastern Desert of Egypt, *Unpublished M. Sc. Thesis*, Geology Dept., Faculty of Science, Tanta University, 88p.

Masoud, A., Masumoto S., Raghavan V., Kajiyama A., and Shiono K. (2002a) Landscape Modeling and Analysis Based on Digital Elevation Models Generated from Topographic Maps: Algorithm and Application on Safaga Area, Red Sea Coast, Egypt. *Journal of Geosciences, Osaka City University*, **45**, pp. 73-87.

Masoud, A., Masumoto, S., Raghavan V., and Shiono K. (2002b) Stream Network and Basin Boundary Extraction Using GRASS GIS:El-Barud Basin, Safaga Area, Red Sea Coast, Egypt. *Geoinformatics*, **13**(4), pp. 205-212.

McCullagh, M. J. (1988) Terrain and surface modeling systems: theory and practice. *Photgrammetric Record*, **12**(47), pp. 747-779.

Moore, I. D., Grayson, R. B., and Ladson, A. R. (1991) Digital terrain modeling: a review of hydrological, geomorphological and biological applications. *Hydrological Processes*, **5**, pp. 3-30.

Noumi, Y., Shiono, K., Masumoto, S., and Raghavan, V. (1999) Generation of DEM from the Topographic Maps, —Utilization of Inter-Contour Information—. Geoinformatics, **10**(4), pp. 235-246.

O'Loughlin, E. M. (1981) Saturation regions in catchments and their relation to soil and topographic properties. *Journal of Hydrology*, **53**, pp. 229-226.

Raafat Masak (1991) "Preliminary report on hazards of the 22-23 October 1990 Floods in the area between Quseir and Ras Gemsa, Red Sea Governorate", In: Development of disaster preparedness, prevention and management planning project (1991): Progress report (1) on: Mitigation of flash flood hazards (August 1989-February 1991). Remote Sensing Center, Academy of Scientific Research & Technology, 160p.

Schumm, S. A. (1956) Evaluation of drainage systems and slopes in Perth Amboy, New Jersey. *Geological*

Society of American Bulletin, **67**(5), pp. 597-646.

Shiono K., Noumi Y., Masumoto S., and Sakamoto M. (2001) Horizon2000: Revised Fortran Program for Optimal Determination of Geologic Surfaces Based on Field Observation Including Equality-Inequality Constraints and Slope Information (in Japanese). *Geoinformatics*, **12**(4), pp. 229-249.

Shiono, K., Wadatsumi, K., and Masumoto, S. (1987) Numerical Determination of the Optimal Geological Surface — A New Gridding Algorithm for Geological Data Including Inequality and Dip Information —. *Joho chishitsu* (*Geological Data Processing*), **12**, pp. 299-328.

Shohami, D. (1997) October 17-18, 1997 Chase Report, (http://israelstorms. netfirms. com/)

Smart, J. (1972) Channel networks. *Advances in Hydroscience*, **8**, pp. 305-346.

Snyder, F. F. (1938) Synthetic unitgraphs. *Transactions of the American Geophysical Union supplement*, Part **2**, p. 447 [Cited in Linsley et al., 1982 and Wilson, 1983].

Strahler, A. N. (1952) Hypsometric (area-altitude) analysis of erosional topography. *Geological Society of America Bulletin*, **63**, pp. 1117-1142.

Tarboton, D. G. (2002) Terrain Analysis Using Digital Elevation Models (TauDEM), http://moose. cee. usu. edu/taudem/taudem. html.

USDA-SCS (1985) National Engineering Handbook, Section 4-Hydrology. Washington.

USGS EROS Data Center (1996) (http://edcwww. cr. usgs. gov/landdaac/gtopo30/gtopo30. html).

U.S. Soil Conservation Service, SCS, (1972) *National Engineering Handbook, Section 4.*, U.S. Department of Agriculture, Washington, DC.

Werner, C. L., Wegmüller, U., Strozzi, T., and Wiesmann, A. (2000) Gamma SAR and Interferometric Processing Software, Proceedings of ERS-ENVISAT Symposium, Gothenburg, Sweden, http://www. gamma-rs. ch/docs/gamma. pdf.

Wolock, D. M. (1993) Simulating the variable-source-area concept of watershed hydrology with TOPMODEL: *USGS Water-Resources Investigation Report* 4124, 33p.

Zangwill, W. I. (1967) Non-linear programming via penalty function. *Management Science*, **13**, pp. 344-358.

Manuscript received August 27, 2003.
Revised manuscript accepted January 8, 2004.